

LHC Beam Loss Monitors

A. Arauzo Garcia; B. Dehning; G. Ferioli; E. Gschwendtner.

CERN, Geneva – CH

Abstract

At the Large Hadron Collider (LHC) a beam loss system will be installed for a continuous surveillance of particle losses. These beam particles deposit their energy in the super-conducting coils leading to temperature increase, possible magnet quenches and damages. Detailed simulations have shown that a set of six detectors outside the cryostats of the quadrupole magnets in the regular arc cells are needed to completely diagnose the expected beam losses and hence protect the magnets.

To characterize the quench levels different loss rates are identified. In order to cover all possible quench scenarios the dynamic range of the beam loss monitors has to be matched to the simulated loss rates. For that purpose different detector systems (PIN-diodes and ionization chambers) are compared.

Presented at DIPAC 2001 – Grenoble– France

13 – 15 May 2001

LHC BEAM LOSS MONITORS

A. Arauzo Garcia, B. Dehning, G. Ferioli, E. Gschwendtner, CERN, Geneva, Switzerland

Abstract

At the Large Hadron Collider (LHC) a beam loss system will be installed for a continuous surveillance of particle losses. These beam particles deposit their energy in the super-conducting coils leading to temperature increase, possible magnet quenches and damages. Detailed simulations have shown that a set of six detectors outside the cryostats of the quadrupole magnets in the regular arc cells are needed to completely diagnose the expected beam losses and hence protect the magnets.

To characterize the quench levels different loss rates are identified. In order to cover all possible quench scenarios the dynamic range of the beam loss monitors has to be matched to the simulated loss rates. For that purpose different detector systems (PIN-diodes and ionization chambers) are compared.

1 LHC PARAMETERS

1.1 Quench levels

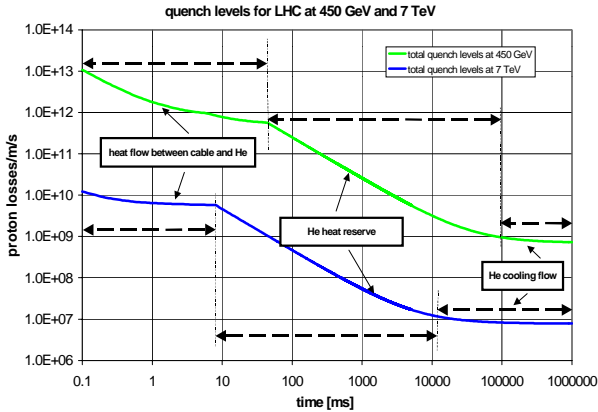


Figure 1: Different quench levels for 450GeV and 7TeV.

Super-conducting magnets can quench if a local deposition of energy due to beam particle losses increases the temperature to a critical value. Figure 1 shows the maximal allowed proton losses/m/s at 450GeV and 7TeV for quenches being reached after different time scales. These quench levels are determined by the coil materials and the coil cooling. The main effects are[1]:

1. At short time scales ($\tau < 50\text{ms}$ at 450GeV, $\tau < 8\text{ms}$ at 7TeV) the maximal allowed proton loss rate is limited by the heat reserve of the cables as well as by the heat flow between the super-conducting cables and the helium.

2. At intermediate time-scales ($\tau > 50\text{ms}$ at 450GeV, $\tau > 10\text{ms}$ at 7TeV) the limited heat reserve of the helium determines the quench levels.
3. The maximal helium flow to evacuate the heat across the insulation defines the allowed proton losses at times above seconds.

The proton loss rate extends over six orders of magnitude. An uncertainty of 50% is considered for the levels.

1.2 Operation conditions

The magnet protection must cover the different filling schemes for LHC shown in Table 1 at injection, ramping and top energy.

Table 1: Different filling schemes for the LHC.

filling scheme	Number of bunches	number of protons/bunch
pilot bunch	1	$5 \cdot 10^9$
TOTEM	36	$1 \cdot 10^{10}$
batch	243	$1 \cdot 10^{11}$
nominal	2835	$1.1 \cdot 10^{11}$

2 SIMULATION OF BEAM LOSSES AND DETECTOR LOCATIONS

With the Monte Carlo code GEANT 3.21 the impact of beam protons on the aperture of the super-conducting magnets has been simulated[2]. In order to detect the beam losses outside the cryostat the shower development in the magnets has been computed in consideration of the main different geometries and magnetic field configurations. These calculations allow determining the suitable positions of the beam loss detectors as well as the needed number of monitors. The results show that a set of six monitors outside the cryostat of the quadrupole magnets in the arc cells are needed to completely diagnose the expected beam loss.

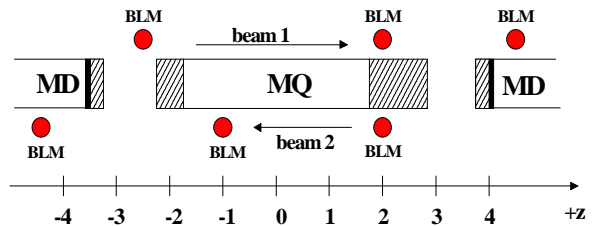


Figure 2: Proposed beam loss monitor locations around the quadrupoles.

The proposed beam loss detector locations in the arc shown in Figure 2 cover aperture limitations in the

quadrupole magnets where the betatronic function has a maximum value and also misalignment errors between the bending and quadrupole magnets. The locations are also optimized to allow distinction between the counter-rotating beams.

The averaged expected shower particles (MIPs) per lost beam proton per cm^2 reaching the detectors are shown in Table 2. The number of protons depend on the magnet configuration and the different monitor locations. The statistical error on the simulation is between 5% and 10%.

Table 2: Simulated shower particles per lost beam proton per cm^2 .

beam energy	MIPs/p/cm ²	
	min	max
450 GeV	$5 \cdot 10^{-4}$	$3 \cdot 10^{-3}$
7 TeV	$8 \cdot 10^{-5}$	$4 \cdot 10^{-2}$

3 BEAM LOSS DETECTORS

The dynamic range of the detection system must be 10^7 ; six orders are due to the quench levels and a factor 10 comes from the sensitivity for low level losses.

In the following sections the performance and the dynamic range of two different beam loss detector systems are investigated; PIN-diodes are compared with ionization chambers at different quench levels.

3.1 Charge threshold counters

PIN-diode beam loss monitors consist of two reverse-biased PIN-diodes mounted face-to-face[3]. Charged particles that cross the two detectors produce a coincidence signal. The dark counts from random coincidences are very low of the order of $10^3/10\text{ms}$. The efficiency of the PIN-diodes for minimum ionizing particles in coincidence is measured to be 35%[4].

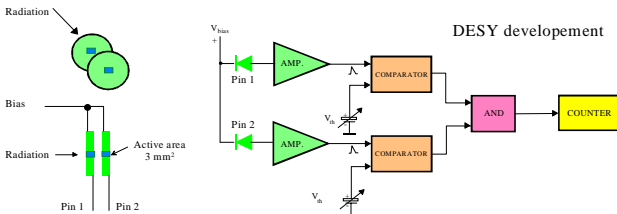


Figure 3: Read-out chain for the two PIN-diodes.

The time resolution of the PIN-diode detectors can be as high as 40MHz. However, since the diodes give per bunch crossing either no hit or only one hit (and not several hits that are proportional to the lost beam protons) the maximum count rate is limited to the bunch passage frequency. This is at nominal LHC conditions $2835 \times 11235.5\text{Hz} = 32\text{MHz}$.

However, this threshold can be raised by almost one order of magnitude when applying Poisson statistics (see in details in [5]).

Table 3 shows the expected PIN-diode counts \mathbf{R} induced by lost protons equivalent to the quench levels in 10ms. \mathbf{R} is calculated according to

$$\mathbf{R} = \mathbf{F} \times \mathbf{P} = \mathbf{F} [1 - e^{-\mathbf{np}}],$$

where \mathbf{F} is the number of bunch passages in a certain time window and \mathbf{P} is the probability for at least one hit in the diodes per bunch crossing. \mathbf{P} depends on the number of lost protons \mathbf{n} per bunch crossing and on the probability \mathbf{p} for a hit in the diodes per one lost proton. We see that the exact knowledge of the number of bunch passages \mathbf{F} is important.

The PIN read-out will saturate, if the counts \mathbf{R} are equal to the number of bunch passages \mathbf{F} (in Table 3 at the pilot filling scheme, at TOTEM for 450GeV and for a batch with 450GeV). In these cases \mathbf{n} or \mathbf{p} is very high and hence the probability \mathbf{P} becomes unity. Applying Poisson statistics is then redundant and no predictions can be made about the number of lost protons and the quench levels.

Table 3: Expected PIN-diode counts in case of a quench caused in 10ms.

filling schemes	max. PIN counts F in 10ms	PIN counts R for a quench caused in 10ms	
		450 GeV	7 TeV
pilot	112	112	112
TOTEM	$4 \cdot 10^3$	$4 \cdot 10^3$	$3.9 \cdot 10^3$
batch	$2.7 \cdot 10^4$	$2.7 \cdot 10^4$	$1.1 \cdot 10^4$
nominal	$3.2 \cdot 10^5$	$1.7 \cdot 10^5$	$1.4 \cdot 10^5$

The saturation effects shown in Table 3 can be improved by taking advantage of the angular distribution of the MIPs that hit the detectors. Using two diodes with a distance of e.g. 2cm and with different sizes (e.g. 10mm^2 and 3mm^2) decreases the probability for hits in the diodes and hence the counting rate (up to a factor 10). Saturation happens then only at the pilot filling scheme.

At the smallest quench level read-out (quench level in 1s at 7TeV, pilot filling scheme) the signal to noise ratio is $S/N = 3 \cdot 10^4$.

3.2 Charge integration counters

The proposed ionization chambers (SPS type) have a surface of 30cm^2 and a length of 30cm. The air-filled detectors are polarized at $V_{\text{bias}} = 800\text{V}$. One MIP produces ~ 2000 electron/ion-pairs. Tests[6] have shown that the response of the ionization chamber is linear up to $10^{12} - 10^{13}$ MIP/s/cm². The maximal expected rate is at the order of 10^{11} MIP/s/cm².

The read-out chain is shown in Figure 4. An Integrator integrates the ionization chamber current during a gate length of 10ms. In case it saturates at 5V within this gate, the capacity of the integrator is discharged and a 12bit counter is incremented. At the end of the 10ms gate the counter is read out and a 12bit ADC samples the integrator output.

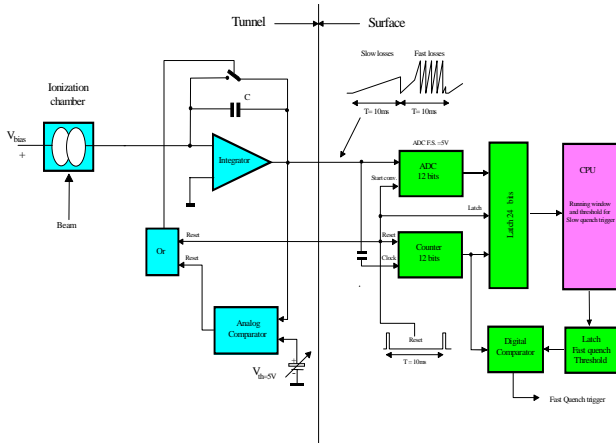
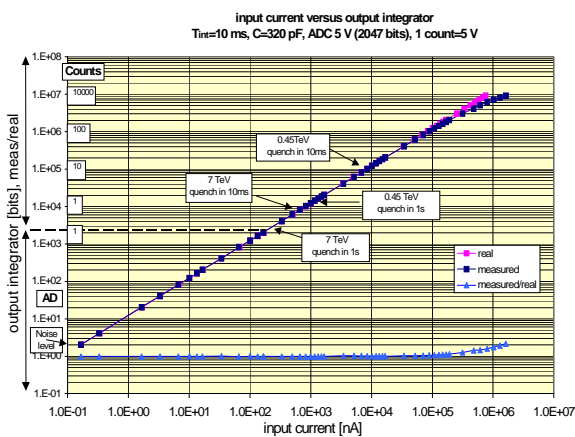


Figure 4: Read-out chain for the ionization chamber.

In case of very large signals the ADC value becomes irrelevant and the counter can be even read out in smaller time intervals (like every turn = 89 μ s). Figure 5 shows the output integrator results in bits depending on the input current relevant for LHC. We see that at very high currents dead-time corrections have to be applied due to the capacitor discharge duration. However, all quench levels are well in the linear range.

The counter together with the ADC allow a very large dynamic range of the order of 10^7 . The time resolution ranges between 0.1ms and several seconds. The noise level is in the range of ± 2 mV, hence the signal to noise ratio for the smallest quench level signal (ie. quench levels reached in 1s at 7 TeV) is $S/N=1.3 \cdot 10^3$.

Figure 5: Integrator output signal for the ionization chamber versus input current.



5 SUMMARY

Table 4 summarizes the characteristics of the PIN-diodes and the ionization chamber.

Since the diodes are 1-hit/no-hit devices they saturate at quenches reached in 10ms for the pilot filling scheme.

Very fast loss detection (1 turn) is not possible due to these saturation effects. The ionization chambers cover all possible filling schemes. Although the diodes have a single bunch loss resolution, this is not of importance for the arc monitors at LHC. In addition the significance is little because of the saturation effects.

The electronics for both detector systems will be installed below the central quadrupole magnet where the radiation dose is expected to be only 5-10 Gy/year[7].

Both detector systems are very reliable. Practical experience from SPS shows that during 12 years of operation no ionization detector elements have been exchanged due to ageing effects. At DESY no PIN-diode detector failures were observed during 8 years of operation.

Comparing the performance of the two detector systems shows that the choice will be mainly driven by cost estimates.

Table 4: Comparison between PIN-diodes and ionization chamber.

PROPERTIES	PIN-diodes	ionization chamber
signal read-out	1-hit/no-hit mode	proportional mode
protection of quenches caused in 10ms	not for pilot	yes
Protection of quenches caused in 1s	yes	yes
read-out resolution	bunch	1 turn (89 μ s)
first turn detection	no	yes
additional needed information	nr. of bunches	-
signal/noise ratio S/N	$3 \cdot 10^4$	$1.3 \cdot 10^3$
cabling	fibre optics	twisted pair cables

ACKNOWLEDGMENTS

We acknowledge the many fruitful discussions about quench levels with Bernard Jeanneret.

REFERENCES

- [1] J. B. Jeanneret et al., LHC Project Report 44, CERN, (1996).
- [2] A. Arauzo Garcia et al., LHC Project Note 213, CERN, (2000).
- [3] K. Wittenburg, Nucl. Instr. and Meth. A 345 (1994) 226-229, (1994).
- [4] F. Ridoutt, Int. Report, PKTR Note No. 91, (1993).
- [5] H. Burkhardt, I. Reichel, SL Note 96-26 OP, (1996).
- [6] V. Agoritsas, MPS-66-23, CERN, (1966).
- [7] C. Fynbo, G. Stevenson, LHC Project Note 251 CERN, (2001).